Supporting Information

Unnatural triazolyl nucleoside stabilizes an abasic site containing DNA duplex equally as the stabilization of a natural A-T pair†

Subhendu Sekhar Bag,* Rajen Kundu and Sangita Talukdar

†Dedicated to Professor Isao Saito on the occasion of his 72nd birthday

Bio-organic Chemistry Laboratory, Department of Chenistry, Indian Institute of Technology Guwahati, Guwahati-781039, Assam, India. Fax: (+)91-361-258-2349.
E-mail: ssbag75@iitg.ernet.in

1. General experimental section (Materials and methods)

The triazolylphenanthrene decorated nucleoside, $^{TPhen}\mathbf{B_{Do}}$, was synthesized following our previous method by azide-alkyne cycloaddition reaction and characterized by ^{1}H NMR, ^{13}C NMR spectra and by HRMS.[1] The starting β-azide was synthesized by a modified method described below to get excellent yield. The nucleoside was incorporated into oligonucleotides via phosphoramidite chemistry using automated DNA/RNA synthesizer following our previous method. In summary, the reagents for DNA synthesis were purchased and used. Mass spectra of oligodeoxynucleotides were determined with a MALDI-TOF MS (acceleration voltage 20 kV, positive mode) with 2′,3′,4′-trihydroxyacetophenone as a matrix. Concentration was measured from molar extinction coefficient at 260 nm at 80 ^{o}C for all ODNs. All aqueous solutions utilized purified water. Reversed-phase HPLC was performed on reverse phase columns (10 × 150 mm, 4.6 × 150 mm) with a chromatograph, using a UV detector, at 254 nm.

Syntheses of oligonucleotides (ODNs) containing $^{TPhen}\mathbf{B_{Do}}$ (ODN **1** and ODN **7**) were performed by a conventional phosphoramidite method on 0.2 μmol scale using an automated DNA/RNA synthesizer. 5'-tritylated deoxytriazolylphenanthrene nucleoside β-cyanoethyl phosphoramidite monomers (0.05 M d$^{TPhen}\mathbf{B_{Do}}$ in anhydrous CH_3CN) and succinyl-linked LCAA-CPG (long chain alkyl amine controlled pore glass) columns with the pore size of 500 Å were used. Standard procedures were followed i.e. trichloroacetic acid in CH_2Cl_2 as detritylation reagent; 0.25 M 4,5-dicyanoimidazole (DCI) in CH_3CN as activator; acetic anhydride in THF as cap A solution; *N*-methylimidazole in THF as cap B solution, and 0.02 M iodine in H_2O/pyridine/THF as the oxidizing solution were used. Natural nucleotides monomers, CPG columns, and all reagents were purchaged and used as received. Extended coupling times (0.05 M in CH_3CN, 5 min) and 1*H*-tetrazole as catalyst were used for the corresponding amidite of d$^{TPhen}\mathbf{B_{Do}}$ monomers. The coupling yield was 90%. The oligomers were detached from solid support and deprotected under standard conditions (conc. aq. NH_3, 55 ^{o}C, 12 h). ODNs were purified by reverse phase HPLC on a 5-ODS-H column (10×150 mm, elution with 50 mM ammonium formate buffer (AF), pH 7.0, linear gradient over 45 min from 3% to 40% acetonitrile at a flow rate 2.0 ml/min). The concentration of each ODN was determined from molar extinction

coefficient at 260 nm at 80 ^{o}C. Mass spectra of ODNs purified by HPLC were determined with a MALDI-TOF mass spectrometer. The concentrations of all the oligonucleotides were measured using the extinction coefficients at 260 nm (ε_{260}) which were calculated with Oligo Analyser (http://eu.idtdna.com). For the triazolylphenanthrene containing building block ($^{TPhen}\mathbf{B_{Do}}$) a ε_{260} value of 28690 was used. The concentration of stock ODN **1** and ODN **7** was 152.3 µM and 138.5 µM respectively.

Complementary natural ODNS (ODN **3-6** and ODN **9-12**) and abasic site containing ODNs (ODN **2** and ODN **8**) were purchased and used as supplied.

2. *Synthesis*

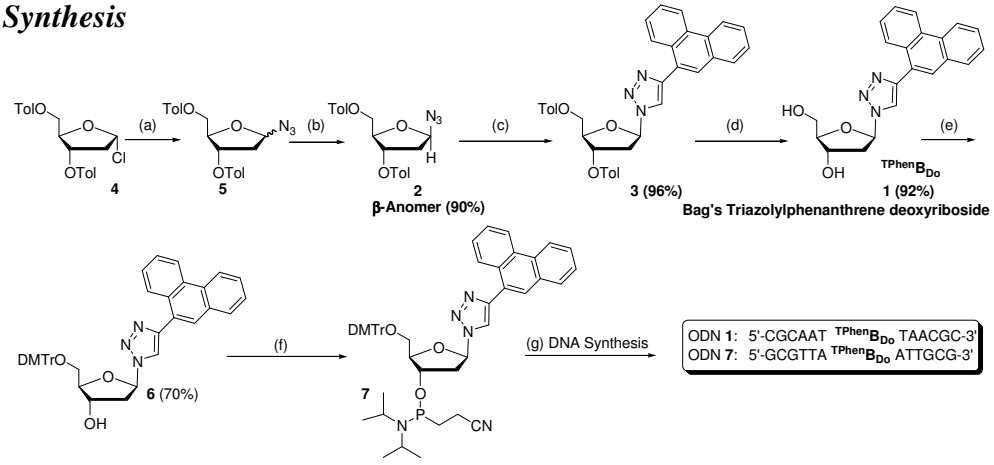

Reagents and condition: (a) CsN_3, DMSO; (b) Column separation; (c) 9-phenanthrene acetylene, $CuSO_4$, Na-Ascorbate, DIPEA, 80 ^{o}C, 12 h; (d) NaOMe/MeOH, r.t.. 12 h (e) DMTrCl, DMAP, Pyridine, 12 h; (f) $(i\text{-}Pr_2N)_2PO(CH_2)_2CN$, DIEA, DCM, rt, 1.5 h; (g) DNA synthesis.

Synthesis of 2-Deoxy-3,5-bis[O-(p-toluoyl)]-β-D-ribofuranosyl azide (2):[1-2] To a solution of cesium azide (CsN_3) (0.350 g, 0.002 mol, 1.2 eq.) in dry DMSO toluyl protected chloro-deoxyribose sugar (0.648 g, 0.0017 mol, 1 eq.) was added at room temperature. The solution was stirred vigorously for 6 hours. After completion of the reaction monitored by TLC the reaction mixture was partitioned between water and EtOAc. The organic layer was washed with water followed by brine solution, dried over Na_2SO_4, and then concentrated. The crude azide obtained was found to be 0.633 g (98%, 0.0016 mmol). The mixture of α- and β-isomers produced in 1 : 10 ratio was then separated by silica gel column chromatography (230-400 mesh) using hexane/EtOAc (20 : 1) mixture as eluting solvent system to isolate β-anomer **2** in 90% yield (0.569 g, 0.0014 mol) and characterized by IR, NMR spectroscopy and mass spectrometry. Yield 90%; ^{1}H NMR ($CDCl_3$, 400 MHz) δ 2.41 (3H, s), 2.42 (3H, s), 4.52-4.61 (5H, m), 5.57-5.59 (1H,

m), 5.72 (1H, t, *J* = 4.8 Hz), 7.22-7.26 (4H, m), 7.9 (2H, d, *J* = 8.4 Hz), 7.98 (2H, d, *J* = 8.4 Hz); ^{13}C NMR ($CDCl_3$, 100 MHz) δ 21.7, 38.9, 64.1, 74.7, 83.7, 92.1, 126.8, 126.9, 129.3, 129.7, 129.9, 144.0, 144.3, 166.2, 166.3. ESI-TOF-MS m/z 418 $[M + Na]^+$.

Synthesis of 1-(2'-deoxy-β-D-ribofuranosyl)-4-(phenanthren-9-yl)-1H-1,2,3-triazole (1, $^{TPhen}B_{Do}$)[1]: To a solution of bis-toluoyl protected β-azido–deoxy ribose sugar (**2**, 0.200 g, 0.0005 mol) in dry THF taken in a round bottom flask fitted with a septum, the anthranyl acetylene (0.154 g 0.00076 mmol, 1.5 equiv) was added under inert N_2-atmosphere. After that, 6 mol% of sodium ascorbate (0.006 g, 0.00003 mol) dissolved in small quantity of water (0.5 ml) followed by 1 mol% of copper sulphate dissolved in water was added to the mixture. The final ratio of THF : H_2O in the reaction mixture was kept at 3:1. After addition of diisopropylethyl amine (DIPEA) to the reaction mixture (0.132 ml, 0.00076 mmol, 1.5 equiv) the solution was heated at 75-80 ^oC overnight with stirring. After full consumption of the starting azide, the reaction mixture was evaporated and partitioned between water and ethyl acetate. The organic layer was washed with water followed by brine solution, dried over Na_2SO_4, and then concentrated in vacuum. The triazolyl product (**3**) was then isolated in pure form by column chromatography (silica-gel 60-120, hexane : EtOAc = 2 : 1) with excellent yield (0.283 g, 0.000475 mol, 95%).[1]

Next, the bis-toluoyl protected triazolyl phenanthrene nucleoside (**3**, 0.200 g, 0.00033 mmol, 1.5 equiv) dissolved in dry methanol was treated with sodium methoxide (0.042 gm, 0.00078 mol, 3.5 equiv) and the resulting reaction mixture was stirred for overnight at room temperature. After completion of the reaction the solution was evaporated and the di-deprotected triazolylphenanthrene nucleoside **1** ($^{TPhen}B_{Do}$) was isolated pure by column chromatography (Silica gel 60-120) using pure EtOAc as eluting solvent and characterized.[1]

Yield 95.0%; mp 166-168 ^oC; IR (KBr) 3364, 1435, 1205, 1121, 1056, 1032 cm^{-1}; ^{1}H NMR (CD_3OD, 400 MHz) δ 2.59-2.64 (1H, m), 2.91-2.96 (1H, m), 3.71 (1H, dd, *J* = 4.4, 11.6 Hz), 3.79-3.82 (1H, m), 4.08-4.1 (1H, m), 4.62-4.65 (1H, m), 6.57 (1H, t, *J* = 5.6, 6.0 Hz), 7.62-7.7 (4H, m), 8.25 (1H, d, *J* = 8.4 Hz), 8.57 (1H, s), 8.78-8.86 (2H, m); ^{13}C NMR (CD_3OD, 100 MHz) δ 42.1, 63.5, 72.5, 90.1, 90.8, 123.9, 124.3, 124.4, 127.4, 128.0, 128.3, 128.4, 128.8, 129.9, 130.2, 131.6, 132.1, 132.3, 132.9, 148.1; HRMS calcd. for $C_{21}H_{20}N_3O_3$ $([M+H]^+)$ 362.1499, found 362.1510.

3. HPLC Trace of Evaluation of α/β-Ratio of Sugar Azide 2

Empower2 software

Reverse-phase HPLC Result

SAMPLE INFORMATION

Sample Name: SGT_αβ-Deoxy D-Ribose Sugar Azide		Acquired By:	System
Sample Type:	Unknown	Sample Set Name:	
Vial:	1	Acq. Method Set:	BHM
Injection #:	1	Processing Method:	TP_1 proc
Injection Volume:	20.00 ul	Channel Name:	W2489 ChA
Run Time:	25.0 Minutes	Proc. Chnl. Descr.:	W2489 ChA 254nm
Date Acquired:	12/24/2012 7:00:43 PM IST		
Date Processed:	12/24/2012 7:55:27 PM IST		

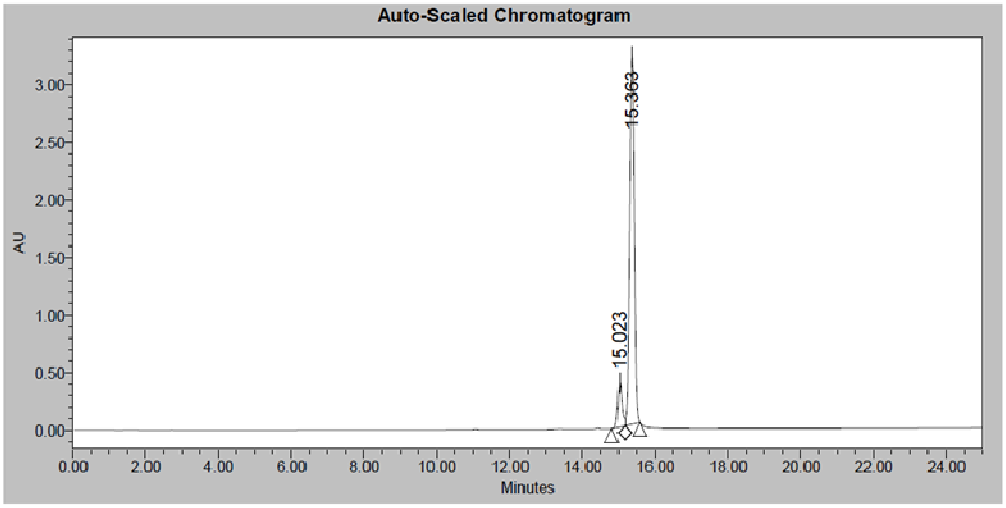

Peak Results

	Name	RT	Area	Height	% Area	
1		15.023	2931632	387311	8.99	α-anomer
2		15.363	29674267	3213898	91.01	β-anomer

α-anomer : β-anomer = 1: 10

Pump Mode: Gradient							
	Time (min)	Flow	%A	%B	%C	%D	Curve
1		1.00	90.0	10.0	0.0	0.0	
2	10.00	1.00	20.0	80.0	0.0	0.0	6
3	23.00	1.00	0.0	100.0	0.0	0.0	6
4	25.00	1.00	0.0	100.0	0.0	0.0	11
A = H_2O and B = CH_3CN; both solvents contain 0.01% Trifluoroacetic acid							

Reported by User: System
Report Method: TP_Result
Report Method ID: 13568
Page: 1 of 1

Project Name: HPLC
Date Printed:
12/24/2012
8:03:55 PM Asia/Calcutta

4. General Spectroscopic Measurements:

4.1. UV-visible measurements: UV-visible spectra of all the ODNs (2.5 µM concentration of each single strand) were measured in 50 mM sodium phosphate buffers (pH 7.0) containing 100 mM sodium chloride and 0.1 mM sodium-EDTA using Shimadzu UV-2550 UV-Visible spectrophotometer. with quartz optical cell of 1.0 cm path length and scanning rate of 0.5 nm with wavelength range of 200-500 nm and slit width of 2 nm.

4.2. Thermal melting temperature (T_m) experiments of the oligonucleotides: The thermal denaturation studies (T_m), absorbance vs. temperature profiles of the duplexes (2.5 µM concentration of each single strand) were measured at 260 nm using Shimadzu UV-2550 UV-Visible spectrophotometer equipped with a Peltier temperature controller using 1 cm path length cell in 50 mM sodium phosphate buffers (pH 7.0) containing 100 mM sodium chloride and 0.1 mM sodium-EDTA. The absorbance of the samples was monitored at 260 nm from 20 to 90 °C with a heating rate of 0.5 °C/min. From these profiles, average method was used to determine T_m values using in built software.

4.3. Calculation of thermodynamic parameters: Thermodynamic parameters were determined by van't Hoff analysis using the relation: $T_m^{-1} = R[ln(C_T)]/\Delta H + \Delta S°/\Delta H°$, where $\Delta H°$ and $\Delta S°$ are the standard enthalpy and entropy changes determined from UV experiments, respectively, R is the universal gas constant and $[C_T]$ is the total strand concentration. From the slope of the plot of $1/T_m$ vs. $\ln(C_T)$, ΔH was calculated and then sustitution of this in the value of intercept yielded ΔS° and then we have calculated ΔG. Thermodynamic parameters (25 °C) were determined from van't Hoff plots using at least four to five different concentrations for each duplex.

4.4. Steady state fluorescence experiments: ODNs solutions were prepared as described in UV-visible and T_m measurement experiments. Fluorescence spectra were recorded using Fluoromax–4 fluorescence spectrophotometer at 25 °C using quartz cell of 1.0 cm path length with a slit width of 3 nm, integration time 0.2 sec and wavelength

range 300-600 nm. Excitation spectra were monitored at 307 (for single standed ODNs) and 319 nm (for duplexes) emission wavelength. Fluorescence emissions were collected exciting the ODNs at the wave length corresponding to their absorption maxima. Steady-state fluorescence emission spectra were recorded at room temperature as an average of five scans using an excitation slit of 3.0 nm, emission slit 3.0 nm, and scan speed of 120 nm/min.The fluorescence quantum yields (Φ_f) were determined using quinine sulphate as a reference with the known Φ_f (0.55)[3] in 0.1 molar solution in sulphuric acid. The following equation was used to calculate the quantum yield,

$$\Phi_S = \Phi_R \frac{Fl_S^{Area}}{Fl_R^{Area}} \frac{Abs_R}{Abs_S} \frac{n_S^2}{n_R^2}$$

where, Φ_R is the quantum yield of standard reference, Fl_S^{Area} (sample) and Fl_R^{Area} (reference) are the integrated emission peak areas, Abs_S (sample) and Abs_R (reference) are the absorbances at the excitation wavelength, and n_S (sample) and n_R (reference) are the refractive indices of the solutions.

The steady state anisotropy experiment was performed with the same fluorescence spectrophotometer at 25 °C using 1 cm path length cell. The fluorescence anisotropy (r) was calculated using the following equation-

$$r = \frac{(I_{VV} - I_{VH}G)}{(I_{VV} + 2I_{VH}G)};\ G = \frac{I_{HV}}{I_{HH}}$$

where, I_{VV} and I_{VH} are the emission intensities when the excitation polarizer is vertically oriented and the emission polarizer is oriented vertically and horizontally respectively. G is the correction factor. The terms I_{HV} and I_{HH} are the emission intensity when the excitation polarization is horizontally oriented and the emission polarization is oriented vertically and horizontally, respectively.

4.5. Time resolved fluorescence experiments: The time resolved fluorescence spectra were obtained using Edinburgh Life spec II time resolved fluorescence

spectrophotometer at 25 °C using 1 cm path length cell in 50 mM sodium phosphate buffers (pH 7.0) containing 100 mM sodium chloride and 0.1 mM sodium-EDTA. 308 nm LED was used as the excitation light source and the monitoring emission wavelength was fixed at 384 nm. The time correlated single photon counting (TCSPC) method was used to calculate the lifetime data. The life time data (Global Analysis) were calculated by the FAST software package (FAST Version 1.9.1. Edinburgh Instruments Ltd.) with fitting range 205 – 4000 channels.

4.6. Circular dichroism (CD) measurement: CD spectra were recorded with JASCO CD J-810 spectropolarimeter equipped with a Peltier thermoelectric type temperature control system (2.5 μM concentration of each strand in 50 mM sodium phosphate, 100 mM sodium chloride, and 0.1 mM sodium-EDTA, pH 7.0, at room temperature). The data were collected using quartz optical cells with a 1.0 cm path length. Measurements were conducted using 2.5 μM of strands in *T*m buffer. Corrections were made for buffer background CD spectra (200-400 nm) were recorded at 25 °C as an average of five scans and with a scan speed of 100 nm/min. The spectral data were analyzed with the spectra manager software.

5. Study of UV-visible and fluorescence photophysical properties of the ODNs

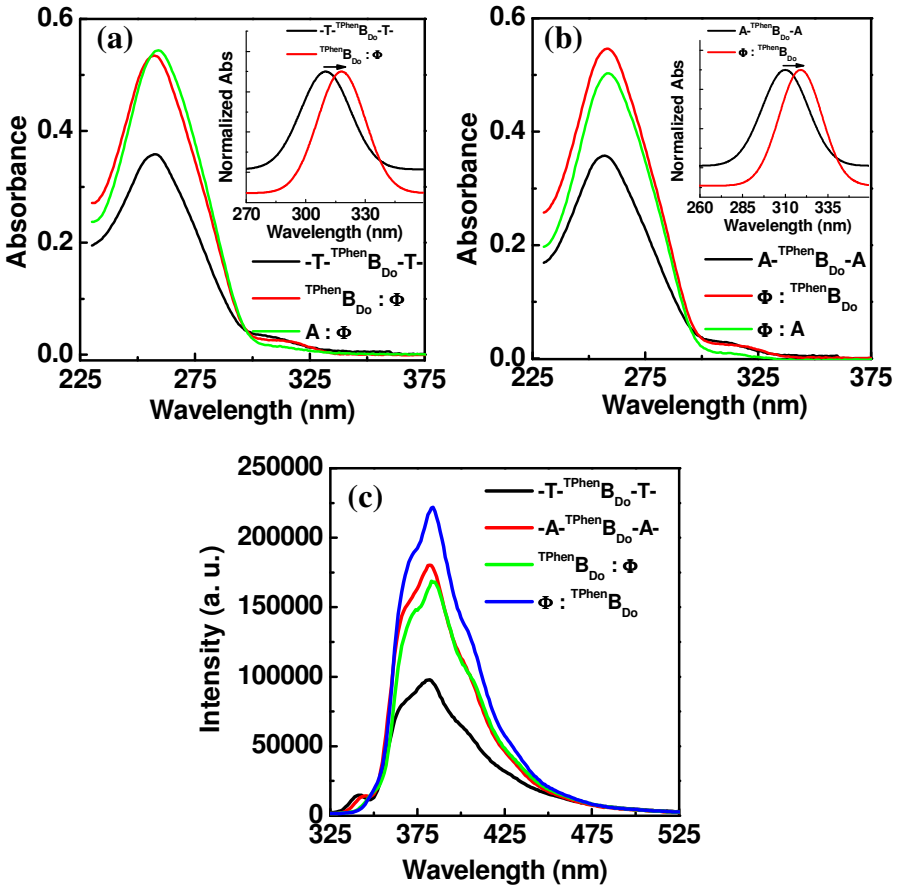

Figure S1: UV-visible spectra of (a) single strand ODN **1** containing $^{TPhen}\mathbf{B_{Do}}$ (T-flanking base), its duplex ($^{TPhen}\mathbf{B_{Do}}$:**Φ**; ODN **1•2**) with abasic site (**Φ**) containing complementary strand ODN **2** and duplex ODN **9•2** (**A** :Φ); (b) single strand ODN **7** containing $^{TPhen}\mathbf{B_{Do}}$ (A-flanking base), its duplex (**Φ**:$^{TPhen}\mathbf{B_{Do}}$; ODN **8•7**) with abasic site (**Φ**) containing complementary strand ODN **8** and duplex ODN **8•3** (**Φ**:**A**). (c) Fluorescence emission spectra of single strand ODNs **1**, **7** and their duplexes with abasic site containing complementary strand (ODN **1•2,** ODN **8•7**). Concentration of each single strand ODNs was 2.5 μM in 50 mM sodium phosphate, 100 mM sodium chloride, 0.1 mM sodium-EDTA, pH 7.0, room temperature.

6. UV-visible and fluorescence photophysical summary table

5'-CGC AAT **X** TAA CGC-3'
3'-GCG TTA **Y** ATT GCG-5'

X : Y	λ_{max} (nm)	Abs.	% Hypochromicity	ε (M^{-1} cm^{-1})	λ_{max} (nm)	Φ_f
-A- $^{TPhen}B_{Do}$ -A-	310	0.0285	--	11400	384	0.039
Φ : $^{TPhen}B_{Do}$	320	0.0207	27.39	8280	384	0.062
-T- $^{TPhen}B_{Do}$ -T-	309	0.0313	--	12520	384	0.021
$^{TPhen}B_{Do}$: Φ	318	0.0224	28.43	8960	384	0.048

7. Time resolved fluorescence summary table

ODNs	X : Y	τ (ns)	χ^2
ODN 1	-T- $^{TPhen}B_{Do}$ -T-	13	1.05
ODN 1•2	$^{TPhen}B_{Do}$: Φ	18	1.13
ODN 7	-A- $^{TPhen}B_{Do}$ -A-	17	1.24
ODN 8•7	Φ : $^{TPhen}B_{Do}$	21	1.20
ODN 1•7	$^{TPhen}B_{Do}$: $^{TPhen}B_{Do}$	15	1.05

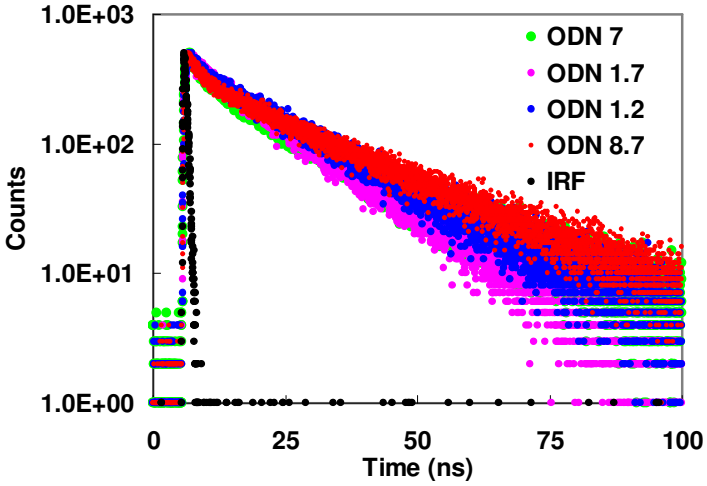

Figure S2: Time resolved fluorescence spectra of the ODNs. Concentration of each single strand ODNs was 10.0 μM in 50 mM sodium phosphate, 100 mM sodium chloride, 0.1 mM sodium-EDTA, pH 7.0, room temperature.

8. Steady state fluorescence anisotropy and polarization summary table

ODNs	X : Y	Anisotropy (x 10^{-2})	Polarization (x 10^{-2})
ODN 1	**-T-$^{TPhen}B_{Do}$-T-**	1.5	2.2
ODN 1•2	**$^{TPhen}B_{Do}$: Φ** (1:1)	3.5	5.1
ODN 1•2	**$^{TPhen}B_{Do}$: Φ** (1:2)	5.8	8.5
ODN 7	**-A-$^{TPhen}B_{Do}$-A-**	1.5	2.2
ODN 8•7	**Φ : $^{TPhen}B_{Do}$** (1:1)	2.7	4.0
ODN 8•7	**Φ : $^{TPhen}B_{Do}$** (1:2)	3.7	5.4

9. Van't Hoff isotherms

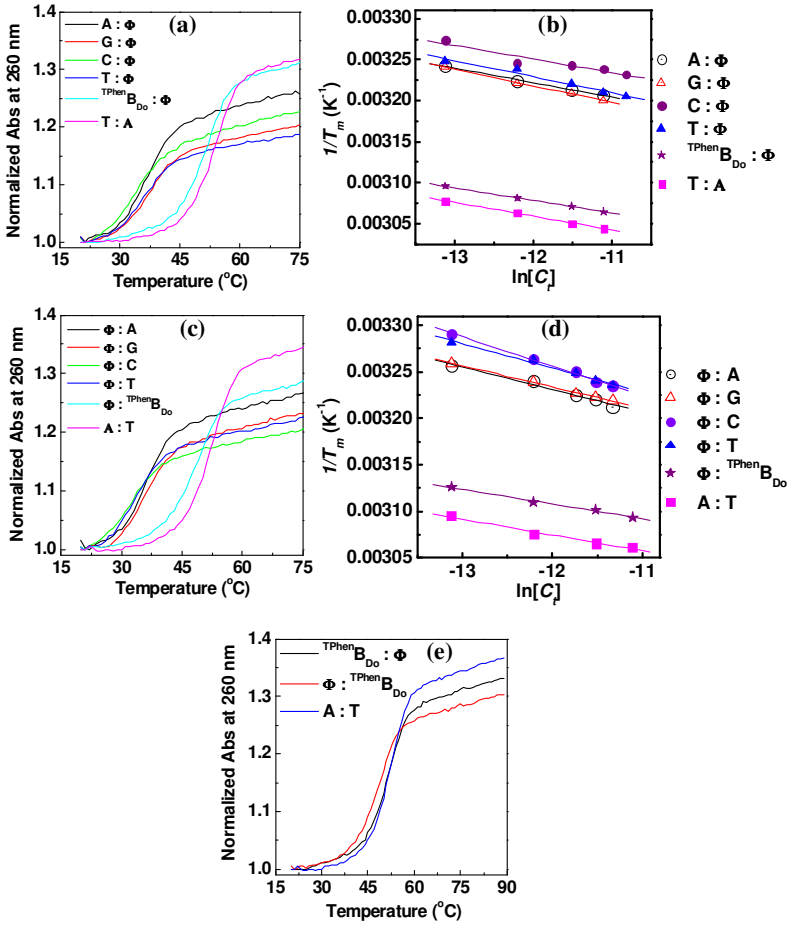

Figure S3: Normalized thermal melting curves (2.5 μM of duplex concentration) and Van't Hoff Isotherms of four to five different concentrations of ODNs-(a-b) ODN **X** : Φ (**X** = A, G, C, T, ^{TPhen}**B$_{Do}$**) and (c-d) ODN **Φ** : **Y** (**Y** = A, G, C, T, ^{TPhen}**B$_{Do}$**). All the solutions were prepared in 50 mM sodium phosphate, 100 mM sodium chloride, 0.1 mM sodium-EDTA, pH 7.0.

10. Summary table of thermodynamic study

ODNs	Sequences	ODNs	Sequences
1.	5'-CGCAAT $^{TPhen}B_{Do}$ TAACGC-3'	**7.**	5'-GCGTTA $^{TPhen}B_{Do}$ ATTGCG-3'
2.	5'-GCGTTA **Φ** ATTGCG-3'	**8.**	5'-CGCAAT **Φ** TAACGC-3'
3.	5'-GCGTTA **A** A TTGCG-3'	**9.**	5'-CGCAAT **A** TAACGC-3'
4.	5'-GCGTTA **G** A TTGCG-3'	**10.**	5'-CGCAAT **G** TAACGC-3'
5.	5'-GCGTTA **C** A TTGCG-3'	**11.**	5'-CGCAAT **C** TAACGC-3'
6.	5'-GCGTTA **T** A TTGCG-3'	**12.**	5'-CGCAAT **T** TAACGC-3'

5'-CGC AAT **X** TAA CGC-3'
3'-GCG TTA **Y** ATT GCG-5'

ODNs	X:Y	T_m	ΔT_m	$-\Delta G^0_{37}$	$-\Delta H^0$	$-\Delta S^0$
1•2	$^{TPhen}B_{Do}$:Φ	52.2	+1	13.44	129.09	373.07
9•2	A:Φ	37.2	-14.0	7.48	111.74	336.32
10•2	G:Φ	37.5	-13.7	7.74	97.56	289.76
11•2	C:Φ	35.1	-16.1	-6.89	-90.5	-269.6
12•2	T:Φ	35.8	-15.4	-7.43	-101.6	-303.9
8•7	Φ: $^{TPhen}B_{Do}$	49.0	-2.2	11.92	125.78	367.27
8•3	Φ:A	35.6	-15.6	7.26	81.97	240.98
8•4	Φ:G	35.7	-15.5	7.2	87.34	258.54
8•5	Φ:C	33.4	-17.8	6.8	63.41	182.63
8•6	Φ:T	33.5	-17.7	6.73	75.97	223.36
9•6	A:T	51.2	--	12.95	117.4	337.1
1•7	$^{TPhen}B_{Do}$:$^{TPhen}B_{Do}$	53.6	+2.4	12.85	107.4	305
1•3	$^{TPhen}B_{Do}$:A	48.5	-2.7	12.09	127.6	372.5
1•4	$^{TPhen}B_{Do}$:G	49.4	-1.8	11.39	106.2	306
1•5	$^{TPhen}B_{Do}$:C	51.3	+0.1	12.72	115.3	331
1•6	$^{TPhen}B_{Do}$:T	50.0	-1.2	12.38	118.9	343.6
9•7	A: $^{TPhen}B_{Do}$	47.1	-4.1	10.87	104.5	301.9
10•7	G: $^{TPhen}B_{Do}$	48	-3.2	12.16	137.2	403.4
11•7	C: $^{TPhen}B_{Do}$	48.3	-2.9	11.57	114.6	332.3
12•7	T: $^{TPhen}B_{Do}$	46.9	-4.3	10.78	110.1	320.5

All samples contained 2.5 µM each strand of DNA, 50 mM sodium phosphate, 100 mM sodium chloride, pH 7.0, with 0.1 mM EDTA room temperature. Units of *ΔG and ΔH* are in kcal/mole, while for *ΔS* is in cal/K/mol. Error in T_m is estimated at ± 0.3°C, and in free energy, ± 5%. ΔT_m = Difference in T_m compared to corresponding natural A:T pair.

11. Circular dichroism (CD) study

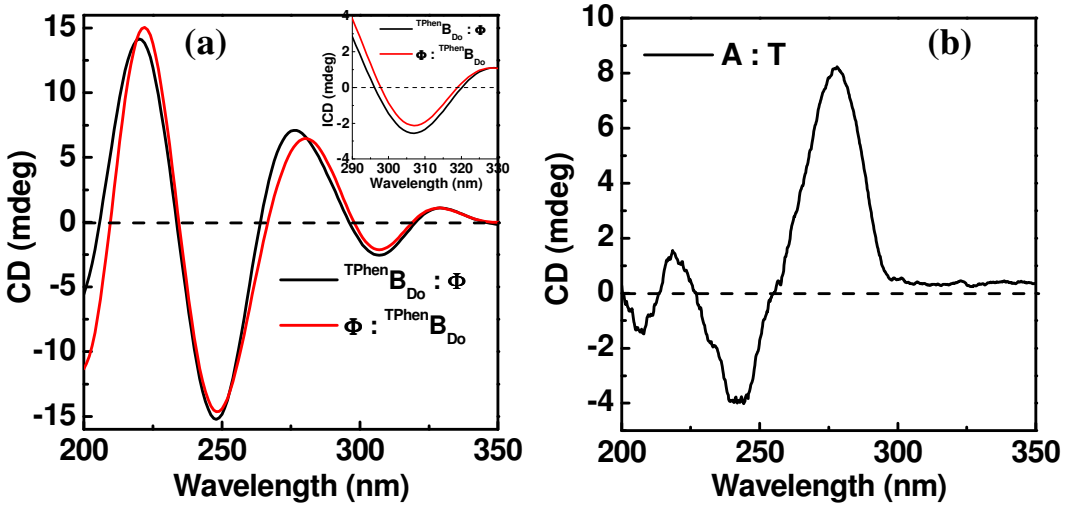

Figure S4: CD spectra of the duplexes (2.5 μM duplex concentration and 50 mM sodium phosphate, 0.1 M sodium chloride, pH 7.0).

12. Macromodel calculations[4]

The conformations of DNA duplexes with triazolylphenanthrene nucleoside opposite to abasic sites were minimized with the Amber* force field using Maestro, version 9.0, Schrödinger Macromodel software.

12.1. Rise between base pairs

Duplex ODNs	Sequences
ODN 1•2	**5'-C_1-G_2-C_3-A_4-A_5-T_6-($^{Tphen}B_{Do}$)$_7$-T_8-A_9-A_{10}-C_{11}-G_{12}-C_{13}-3'** **3'-G_{26}-C_{25}-G_{24}-T_{23}-T_{22}-A_{21}-(Φ)$_{20}$-A_{19}-T_{18}-T_{17}-G_{16}-C_{15}-G_{14}-5'**
ODN 8•7	**5'-C_1-G_2-C_3-A_4-A_5-T_6---------(Φ)$_7$-------T_8-A_9-A_{10}-C_{11}-G_{12}-C_{13}-3'** **3'-G_{26}-C_{25}-G_{24}-T_{23}-T_{22}-A_{21}-($^{Tphen}B_{Do}$)$_{20}$-A_{19}-T_{18}-T_{17}-G_{16}-C_{15}-G_{14}-5'**

X : Y	Rise	Å
$^{TPhen}B_{Do}$: Φ	T_6—($^{Tphen}B_{Do}$)$_7$	3.4–3.5
$^{TPhen}B_{Do}$: Φ	($^{Tphen}B_{Do}$)$_7$—T_8	3.3–3.5
Φ : $^{TPhen}B_{Do}$	A_{21}—($^{Tphen}B_{Do}$)$_{20}$	3.3 – 3.6
Φ : $^{TPhen}B_{Do}$	($^{Tphen}B_{Do}$)$_{20}$—A_{19}	3.3 – 3.5

12.2. Macromodel derived structures

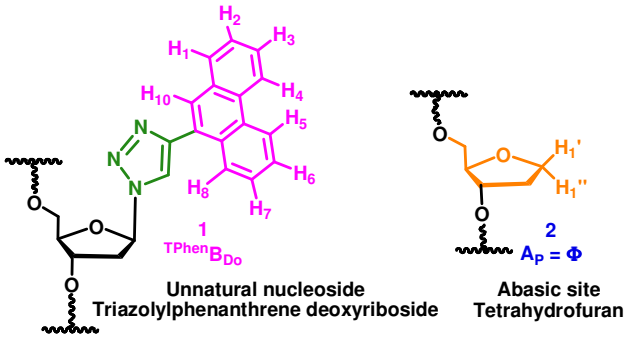

The Amber* optimized geometries of the duplexes ODN **1•2** (**$^{Tphen}B_{Do}$-Φ**) and ODN **8•7** (**Φ-$^{Tphen}B_{Do}$**) showed that all both of them are right–handed helix with all residues having *anti* glycosidic bond and C2'-*endo*/C3'-*exo* sugar conformations. Helical rise values [Rise T_6/ (**$^{Tphen}B_{Do}$**)$_7$: 3.4–3.5 Å; and Rise (**$^{Tphen}B_{Do}$**)$_7$/ T_8: 3.3–3.5 Å] are close to those observed in B–form DNA (3.4 Å), with slight deviations at and near the abasic site (Table 3). In both of the structures the triazolylpyrene residue resided inside the helix. The abasic site residue was also found to be intrahelical with C2′-*endo* sugar conformation in both the duplexes. The C1′ and C2′ of abasic residues in **$^{Tphen}B_{Do}$–Φ** duplex are close to the H_3-H_4-H5 edges of its aromatic partner, triazolylphenanthrene (Fig. S5) while H2-H3 edges of triazolyl phenanthrene are in close proximity with C1′ and C2′ of abasic residues of **Φ-$^{Tphen}B_{Do}$** duplex.

In **$^{Tphen}B_{Do}$–Φ** duplex the H3-edge pointed toward the C1'-*β-H* and C2'-*β-H* of abasic site with distance 3.57 Å, and = 3.10 Å respectively. Also, H4-edge pointed toward the C1'-*β-H* and C2'-*β-H* of abasic site with distance 2.40 Å,and 2.96 respectively. Moreover, H5-edge pointed toward the C1'-*β-H* of abasic site with distance only 3.04 Å. In the same duplex H6-H7 pointed toward minor groove side and H1-H2 pointed towards major groove side.

In **Φ-$^{Tphen}B_{Do}$** duplex the H2-edge pointed toward the C2'-*β-H* of abasic site with distance 2.70 Å. Also, H3-edge pointed toward the C1'-*β-H* of abasic site with distance 2.42 Å. In the same duplex H10 pointed toward minor groove side while H5-H6 pointed towards major groove side.

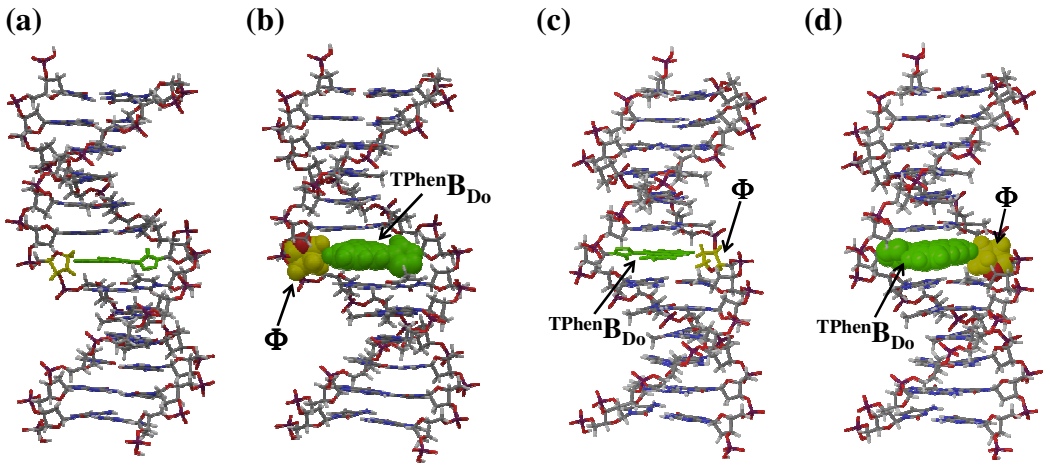

Figure S5. Amber* optimized geometry of the duplexes $^{Tphen}\mathbf{B_{Do}}$-**Φ** (a-b) and **Φ**-$^{Tphen}\mathbf{B_{Do}}$ (c-d). The pictures show the $^{Tphen}\mathbf{B_{Do}}$ residues in green and the abasic sites in yellow colour.

When viewed from the helical axis of the duplex $^{Tphen}\mathbf{B_{Do}}$**–Φ**, it was observed that the triazole ring involved in stacking with flanking T_6 residue of same strand in T-shaped fashion. The full part of triazolyl phenanthrene stack extensively with the flanking T_8 residue of the same strand (intrastrand stacking). Moreover, phenanthrene moiety fully stacked with both A_{19} and A_{21} bases in the tetrahydrofuran-containing strand (interstrand stacking) (Fig. S6).

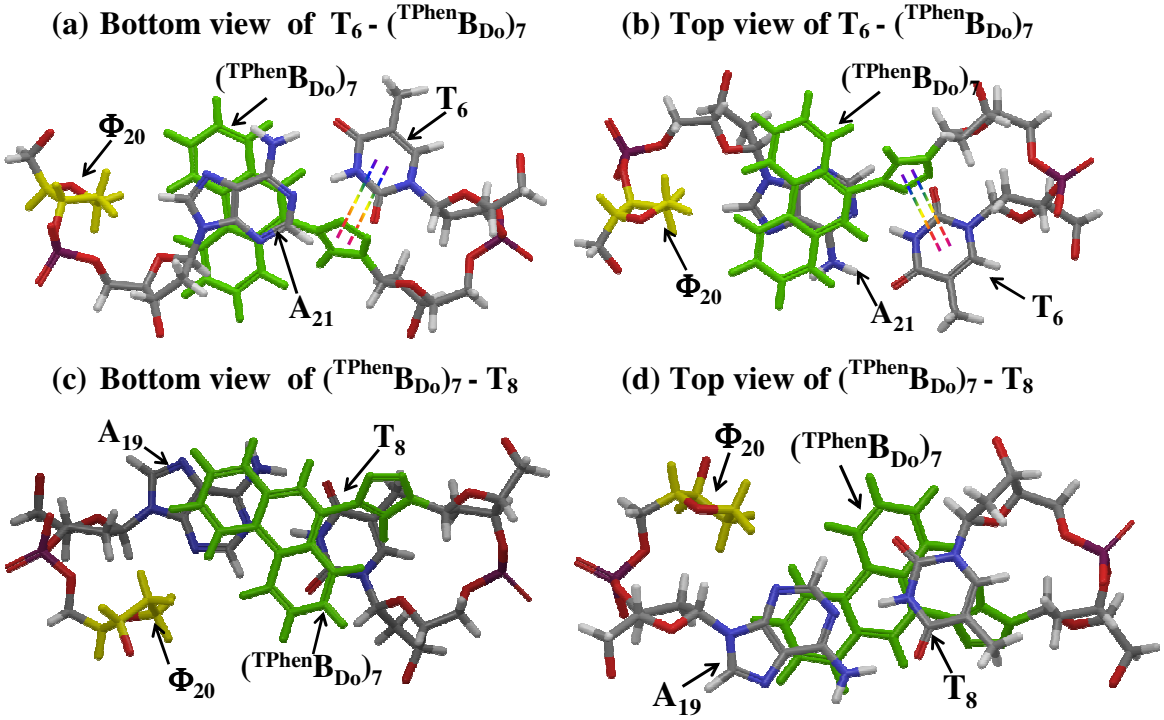

Figure S6. Amber* optimized and helical axis view of the (^{Tphen}**B**$_{Do}$-**Φ**) duplexes showing both the interstrand and intrastrand stacking interactions of ^{Tphen}**B**$_{Do}$ and the bases inside the duplexes. The pictures show the ^{Tphen}**B**$_{Do}$ residues in green and the abasic sites in yellow coloure.

When viewed from the helical axis of the duplex **Φ**-^{Tphen}**B**$_{Do}$, it was observed phenanthrene moiety fully stacked with flanking A_{21} and partially stacked with flanking A_{19} bases in the same strand (intrastrand stacking). However, only one benzene ring of phenanthrene partially stacked with T_8 residue (interstrand stacking) and no interstrand stacking was observed with T_6 residue of tetrahydrofuran–containing strand (interstrand stacking) (Fig. S7).

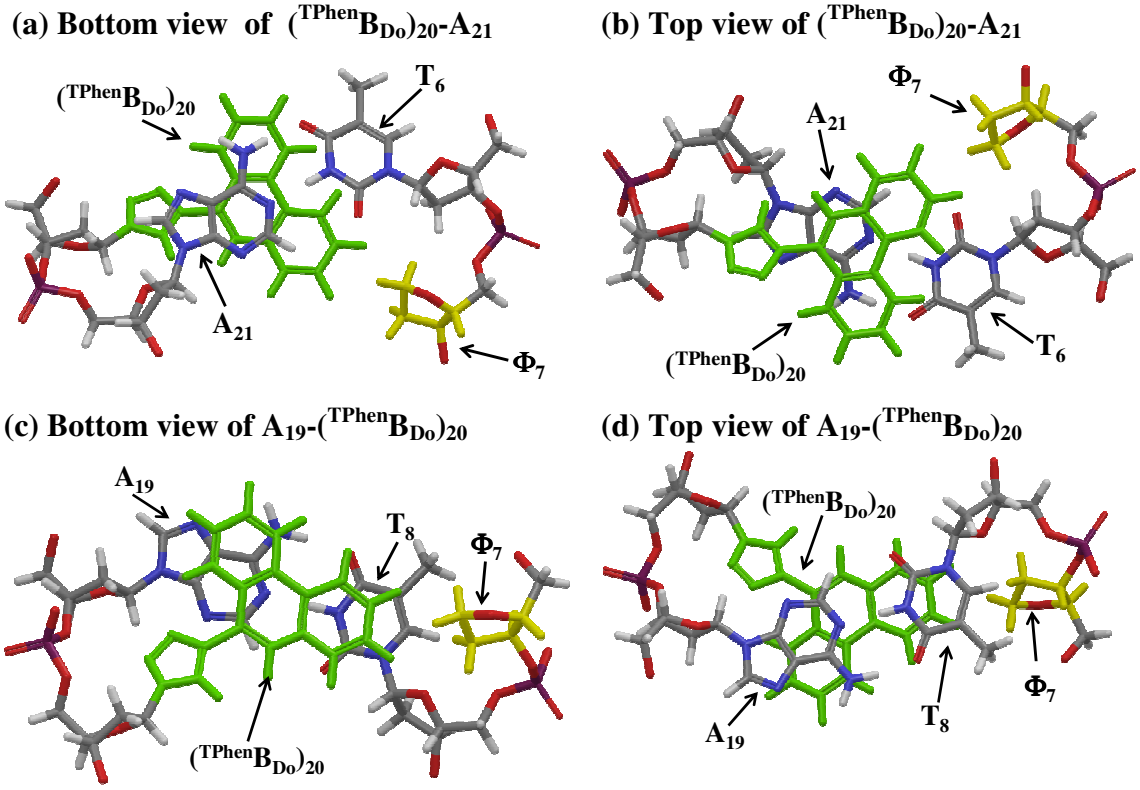

Figure S7. Amber* optimized and helical axis view of the (**Φ-**^{Tphen}**B$_{Do}$**)-duplexes showing both the interstrand and intrastrand stacking interactions of ^{Tphen}**B$_{Do}$** and the bases inside the duplexes. The pictures show the ^{Tphen}**B$_{Do}$** residues in green and the abasic sites in yellow coloure.

The space-filling models revealed that the size of the triazolylphenanthrene (248 Å^2) is comparable to that of natural A-T pair (273 Å^2) and is sufficient enough to establish tight Van der Waals contacts with the abasic site residue in the opposing strand.[5] In the case of the ^{Tphen}**B$_{Do}$–Φ** duplex (**1.2**), there is negligible gap within the ^{Tphen}**B$_{Do}$–Φ** pair when viewed from major groove of the duplex but a small space was seen when viewd from minor groove side (Fig. S8a-b).

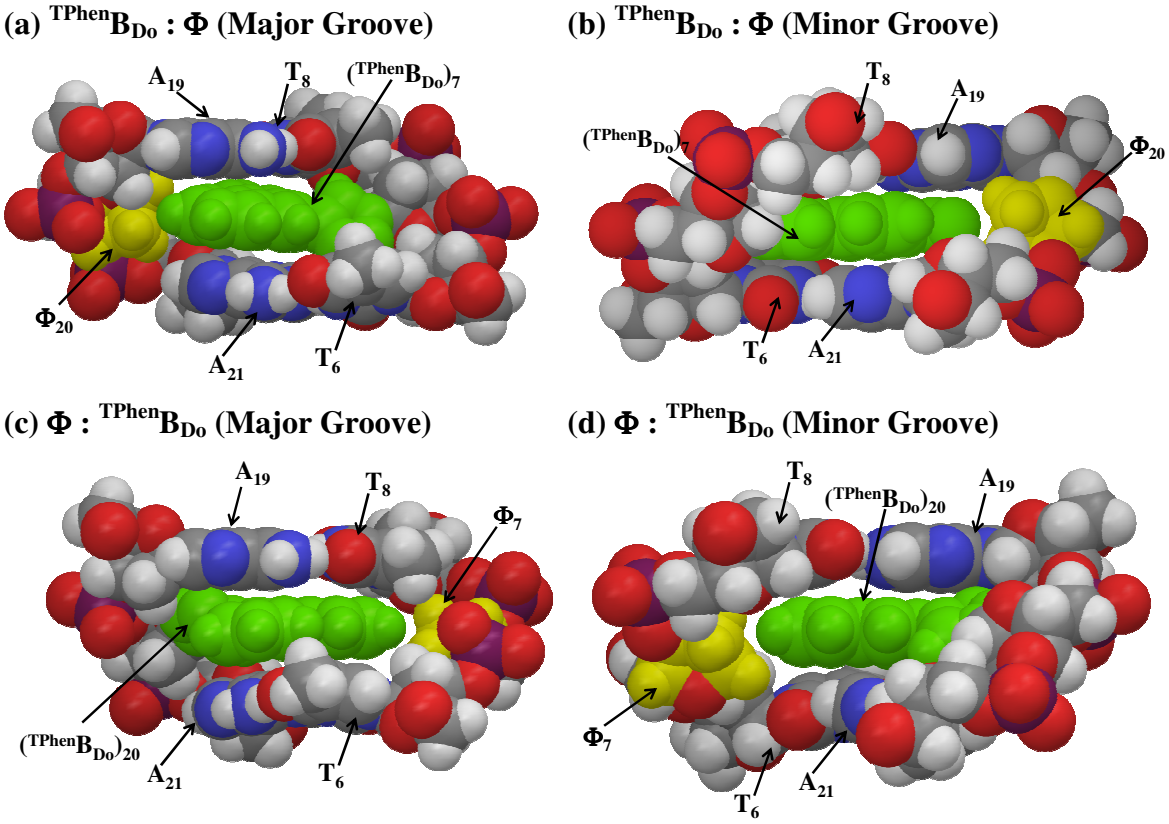

Figure S8. Spacefilling model of the $^{Tphen}B_{Do}$–Φ (a-b) and Φ–$^{Tphen}B_{Do}$ (c-d) duplexes and flanking base pairs with the prominent major groove (left) and minor groove (right). The pictures show the $^{Tphen}B_{Do}$ residues in green and the abasic sites in yellow coloure.

However, a small empty space is present in the Φ–$^{Tphen}B_{Do}$ duplex structure when viewed from both the grooves. As a result, percent of the triazolylphenanthrene surface accessible to solvent in the Φ–$^{Tphen}B_{Do}$ (**8.7**)-duplex is more than the $^{Tphen}B_{Do}$–Φ duplex. Therefore, Φ–$^{Tphen}B_{Do}$ duplex is conformationally more mobile than $^{Tphen}B_{Do}$–Φ duplex to accommodate a water molecule after a minor adjustment of the structure. Comparatively more flexible nature of the Φ–$^{Tphen}B_{Do}$ duplex is probably the cause of less stability of the duplex compared to the duplex $^{Tphen}B_{Do}$–Φ (Fig. S8c-d).

12. References

1. S. S. Bag, S. Talukdar, K. Matsumoto and R. Kundu, *J. Org. Chem.*, **2013,** *78,* 278.
2. (a) Štimac, A.; Leban, I.; Kobe, J. *Synlett.* **1999**, 1069. (b) Štimac, A.; Kobe, J. *Carbohydrate Res.* **2000***, 329*, 317. (c) Guezguez, R.; Bougrin, K.; Akri, K. E.; Benhida, R. *Tetrahedron Lett.* **2006**, *47*, 4807. (d) Chittepu, P.; Sirivolu, V. R.; Seela, F. *Bioorg. Med. Chem.* **2008**, *16*, 8427. (e) Malnuit, V.; Duca, M.; Manout, A.; Bougrin, K.; Benhida, R. *Synlett* **2009**, 2123. (f) Kolganova, N. A.; Florentiev, V. L.; Chudinov, A. V.; Zasedatelev, A. S.; Timofeev, E. N. *Chem. Biodivers.* **2011**, *8*, 568.
3. W. H. Melhuish, *J. Phys. Chem*., **1961**, *65*, 229.
4. Maestro, version 9.0, Schrödinger, LLC, New York, NY, **2009**.
5. T. J. Matray and E. T. Kool, *J. Am. Chem. Soc.*, **1998**, *120*, 6191.

13. ^{1}H NMR spectra of β-azide **2**

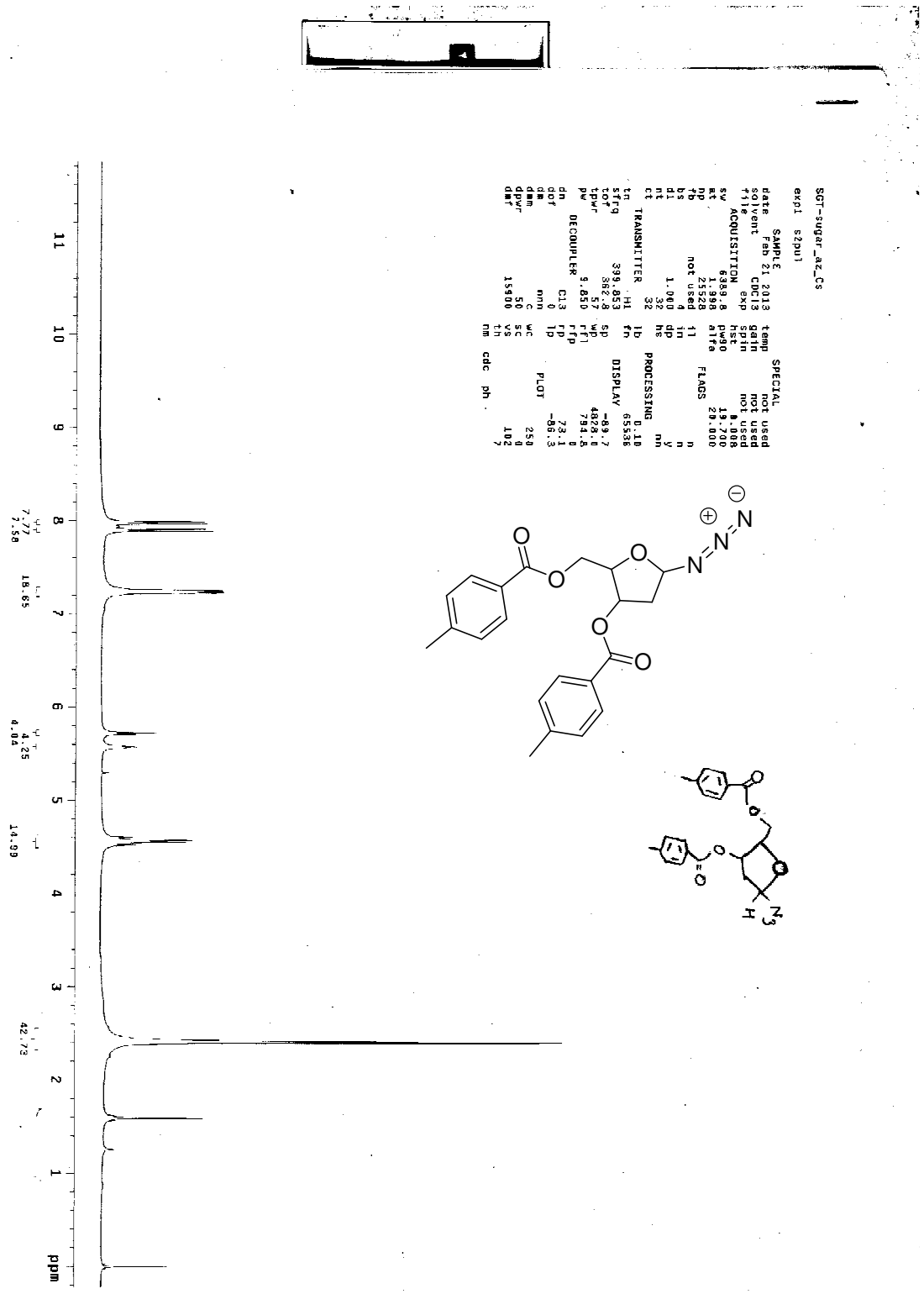

Figure S9: ^{1}H NMR spectra of synthesized azide **2**.